Earth Surface Processes and Landforms
Earth Surf. Process. Landforms **24**, 1173–1188 (1999)

A TWO-DIMENSIONAL MODEL FOR SUSPENDED SEDIMENT TRANSPORT IN THE SOUTHERN BRANCH OF THE RHINE–MEUSE ESTUARY, THE NETHERLANDS

MARJOLEIN VAN WIJNGAARDEN*

**Ministry of Transport, Public Works and Water Management, National Institute for Inland Water Management and Waste Water Treatment (RIZA), Van Leeuwenhoekweg 20, 3316 AV Dordrecht, The Netherlands*

Received 30 January 1998; Revised 6 January 1999; Accepted 9 February 1999

ABSTRACT

For the southern branch of the Rhine–Meuse estuary, The Netherlands, a two-dimensional horizontal suspended sediment transport model was constructed in order to evaluate the complicated water quality management of the area. The data needed to calibrate the model were collected during a special field survey at high river runoff utilizing a number of techniques: (1) turbidity probes were used to obtain suspended sediment concentration profiles; (2) air-borne remote sensing video recordings were applied in order to obtain information concerning the spatial distribution of the suspended sediment concentration; (3) an acoustic probe (ISAC) was used to measure cohesive bed density profiles and (4) an *in situ* underwater video camera (VIS) was deployed to collect video recordings of the suspended sediment. These VIS data were finally processed to fall velocity and diameter distributions and were mainly used to improve insight into the relevant transport processes, indicating significant erosion of sand from the upstream Rhine branch. For quantitative calibration of the model, the data from the turbidity profiles were used. Sedimentation and erosion were modelled according to Krone and Partheniades. The model results showed a good overall fit to the measurements, with a mean absolute error of 18 per cent (standard fault = 1 per cent), corresponding to concentrations of about 0·020 (upstream) to 0·005 kg m^{-3} (downstream). The overall correlation between observed and simulated suspended sediment concentrations was 0·85. The remote sensing video recordings were used for a qualitative calibration of the model. The distribution pattern of the suspended sediment on these photos was reproduced quite well by the model. However, a more accurate calibration technique is needed to enable the use of aerial remote sensing as a quantitative calibration method. Copyright © 1999 John Wiley & Sons, Ltd.

KEY WORDS: modelling; suspended sediment; remote sensing; Rhine–Meuse estuary

INTRODUCTION

The rivers Rhine and Meuse form a combined estuary in the southwestern part of The Netherlands. This estuary is highly regulated by control of river inflows, maintenance dredging of shipping channels and regulation of the river channels through groynes. The estuary has a complex layout as is shown in Figure 1. In the northern outlet (Rotterdam Waterway) of the estuary the important Rotterdam Harbour is situated. The southern part of the estuary consists of the Haringvliet and Hollandsch Diep. These former tidally influenced areas gradually turned into freshwater lakes after the closure of the Haringvliet in 1970 by the Haringvliet Sluices. There is a manipulation programme for these sluices which guarantees a minimum flow (1500 m^3 s^{-1}) through the northern outlet of the estuary, the Rotterdam Waterway. Only during higher (>1700 m^3 s^{-1}) Rhine discharges (approximately 60 per cent of the year) are the Haringvliet Sluices opened, but only during low tide.

Owing to the construction of these sluices, a large sedimentation area has been created in the southern part of the estuary, with a length of over 40 km and a width of 1–4 km. The contaminated silt and clay particles that have been deposited in the area over the last 25 years have severe effects on the water quality in the area

* Correspondence to: M. Van Wijngaarden, Ministry of Transport, Public Works and Water Management, RIZA, Van Leeuwenhoekweg 20, 3316 AV Dordrecht, The Netherlands. E-mail: m.vwijngaarden@riza.rws.minvenw.nl

CCC 0197-9337/99/131173–16 $17.50

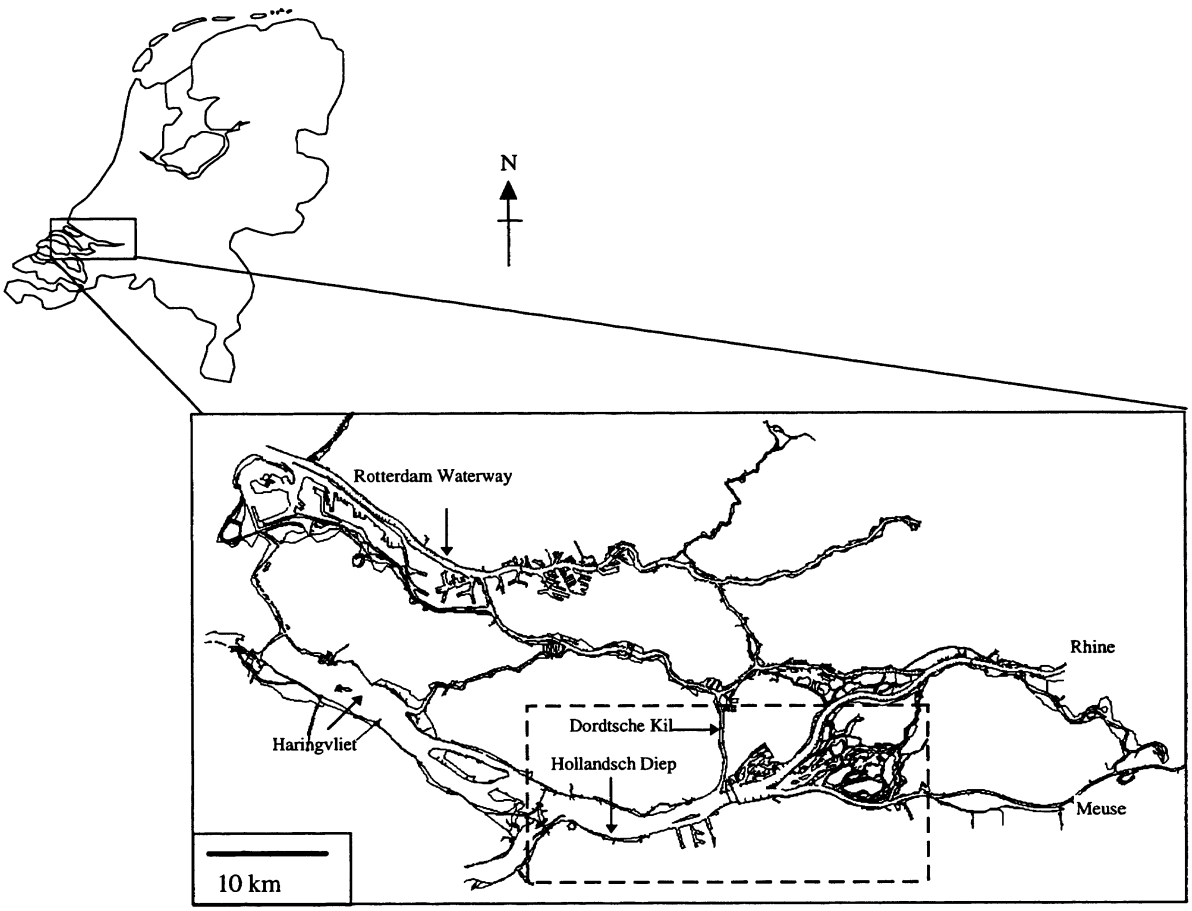

Figure 1. The Rhine–Meuse estuary in The Netherlands and study area of the WAQUA model (within dashed lines)

(Van Eck *et al.*, 1997). The water management presently involves the possible remediation of (parts of) the area.

In order to study the behaviour of the transported sediment and the effectiveness of possible remediation, a one-dimensional model (ZWENDL-DELWAQ) is currently used. This model gives a reasonably accurate prediction of the amount of material deposited (Van Wijngaarden and Ludikhuize, 1998). However, a two-dimensional horizontal (2DH) sediment transport model could provide important information on the pathways of the suspended sediment and eventually on the spatial variability in the thickness of the cohesive bed sediments. This is important information with respect to dredging activities. In this case study a 2DH sediment transport model of the southern part of the estuary, based on the hydrodynamic model WAQUA (Leendertse *et al.*, 1981), will be constructed and calibrated.

THE SEDIMENT TRANSPORT MODEL

WAQUA

The WAQUA model is a general water quantity modelling framework which solves the shallow water equations as its governing hydraulic equations. The WAQUA model, as used in this study, uses a rectilinear

staggered grid with a spacing of 100 m. The model calculations were carried out using an alternating direction implicit scheme (ADI) and a time step of 1 min. Detailed technical information about the WAQUA model can be found in the user's guide (EDS, 1998).

In this study, the WAQUA model was applied to the southern part of the Rhine–Meuse estuary, called the 'WAQUA-ZUIDRAND-OOST' model. The model has three upstream boundaries, corresponding to the rivers Rhine, Meuse and the Dordtsche Kil, and one downstream boundary, at the border between the Haringvliet and Hollandsch Diep. The model study area is shown in Figure 1. The WAQUA-ZUIDRAND-OOST model was extensively calibrated and verified over a wide range of discharges and tidal situations (Collard, 1991).

DELWAQ

DELWAQ is a water quality modelling framework in which an extensive set of options, such as possibilities for calculations on eutrophication, heavy metal transport and suspended matter, are incorporated for use in combination with a one-, two- or three-dimensional hydrodynamic model (Delft Hydraulics, 1994). The sediment transport model used is a general application of DELWAQ on suspended sediment transport. With this model the suspended sediment transport is calculated based on the WAQUA results using the same model layout (see next section for more details). A sensitivity analysis and calibration of this suspended sediment model were carried out for the complete southern branch of the Rhine–Meuse estuary for a situation with an annual average discharge (Collard, 1992).

WAQUA-DELWAQ application

For this study, the WAQUA-ZUIDRAND-OOST model was combined with DELWAQ in order to calculate the suspended sediment transport in the study area. In a first attempt with this model, Verbeek *et al.* (1993) simulated spatial distribution patterns in the study area, linking the WAQUA-ZUIDRAND-OOST model to a DELWAQ-temperature module. With this model, the temperature distribution as a result of the drainage of cooling water into the area was simulated. As calibration data, recordings of a TIR linescanner were used. As this model calibration needed further improvement, the study presented in this paper on suspended sediment transport was initiated.

The DELWAQ suspended sediment model uses three fractions: fine cohesive sediment, flocculated cohesive sediment and fine non-cohesive sediment, the latter being fine sand. There is an active layer (the water column) and an inactive layer (the bed) in the model. The transport between the model compartments in x and y directions is calculated using the advection-diffusion equation (see Equation 1) with two source terms, sedimentation (S) and erosion (E):

$$\frac{\partial hC}{\partial t}+\frac{\partial huC}{\partial x}+\frac{\partial}{\partial x}\left(hD_x\frac{\partial C}{\partial x}\right)+\frac{\partial hvC}{\partial y}+\frac{\partial}{\partial y}\left(hD_y\frac{\partial C}{\partial y}\right)=\left(\sum_1^3 E_i-\sum_1^3 S_i\right) \tag{1}$$

where C = depth-integrated suspended sediment concentration (kg m^{-3}); x,y = horizontal and vertical co-ordinates respectively (m); u = flow velocity in x direction (m s^{-1}) v = flow velocity in y direction (m s^{-1}) t = time (s) h = water depth (m); D_x = diffusion constant in x direction (m^2 s^{-1}); D_y = diffusion constant in y direction (m^2 s^{-1}); $\sum_1^3 E_i$ = sumof the erosion flux E_i of the three sediment fractions (kg m^{-2} s^{-1}); $\sum_1^3 S_i$ = sumof sedimentation flux S_i of the three sediment fractions (kg m^{-2} s^{-1}).

The diffusion constant is, in a simplified form of the Elder (1959) formula, assumed to be linearly dependent on the flow velocity, both in x and y directions. In order to include diffusion initiated by wind forces, mostly occurring in shallow areas, both diffusion constants have a fixed lower boundary of 0·25 cm^2 s^{-1}. In practice, this means that mixing in the longitudinal direction is mainly driven by advection, whereas in the transverse direction, diffusion becomes dominant.

The formulations applied for sedimentation and erosion are rather empirical; for erosion the Partheniades (1965) formula was applied (Equation 2) and the Krone (1962) formula was used to describe sedimentation (Equation 3). Both processes are calculated for each sediment fraction (i):

$$\text{if } \tau < \tau_{\mathrm{e},i}: \quad E_i = 0$$
$$\text{if } \tau > \tau_{\mathrm{e},i}: \quad E_i = f_i M_i \left(\left(\frac{\tau}{\tau_{e,i}} \right) - 1 \right) \tag{2}$$

$$\text{if } \tau > \tau_{\mathrm{s},i}: \quad S_i = 0 \tag{3}$$
$$\text{if } \tau < \tau_{\mathrm{s},i}: \quad S_i = w_{s,i} C_i \left(1 - \left(\frac{\tau}{\tau_{sj}} \right) \right)$$

where M_i = rate of erosion of fraction i (kg m^{-2} s^{-1}), τ = bottom shear stress (N m^{-2}), $\tau_{e,i}$ = critical bottom shear stress for erosion of fraction i (N m^{-2}), $\tau_{s,i}$ = critical bottom shear stress for sedimentation of fraction i (N m^{-2}) C_i = suspended sediment concentration for fraction i (kg m^{-3}), $w_{s,i}$ = settling velocity for fraction i (m s^{-1}), f_i = size of fraction i in bed layer.

The equations employed assume that sedimentation is positively correlated to the concentration of suspended sediment in the water column and negatively correlated to the bottom shear stress. On the other hand, erosion is positively correlated to the bottom shear stress, while during erosion the three sediment fractions will be released by the ratio in which they occur in the bottom.

The 2DH approach assumes that the suspended sediment is homogeneously distributed within the water column; this seems to be a reasonable assumption as this is supported by previous measurements of cohesive sediment in the study area (Verbeek and Jansen, 1993). For the suspended sediment transport calculations in DELWAQ, in this study a second order Lax-Wendroff scheme was used, with a time step of 1 min.

FIELD MEASUREMENTS

Methodology

The confluence area of the Meuse and the Rhine is rather complex: two streams with a different suspended sediment concentration are slowly mixed. The mixing process can best be studied during high river discharges, because of the high, and therefore readily measurable, suspended sediment concentrations. For the calibration of the model a field survey was carried out at a high river runoff of about 4500 m^3 s^{-1}. From a sensitivity analysis with the model it was found that the measurements should be conducted over a length of about 20 km throughout the southern branch of the estuary in order to get a statistically correct resolution for the calibration of the model parameters. In practice this meant that the measurements were carried out from the confluence area of the Rhine and Meuse down to the border of the Hollandsch Diep and Haringvliet. The survey took place on 23 and 24 March 1995 from 8·00 to 16·00 on both days. On those days the Rhine discharge was around 5500 m^3 s^{-1} (yearly average 2300 m^3 s^{-1}) and the discharge of the Meuse around 700 m^3 s^{-1} (yearly average 230 m^3 s^{-1}).

A number of techniques were used in order to obtain an integrated view of the transport processes in the study area. Both at the model boundaries and at several locations throughout the study area measurements were carried out.

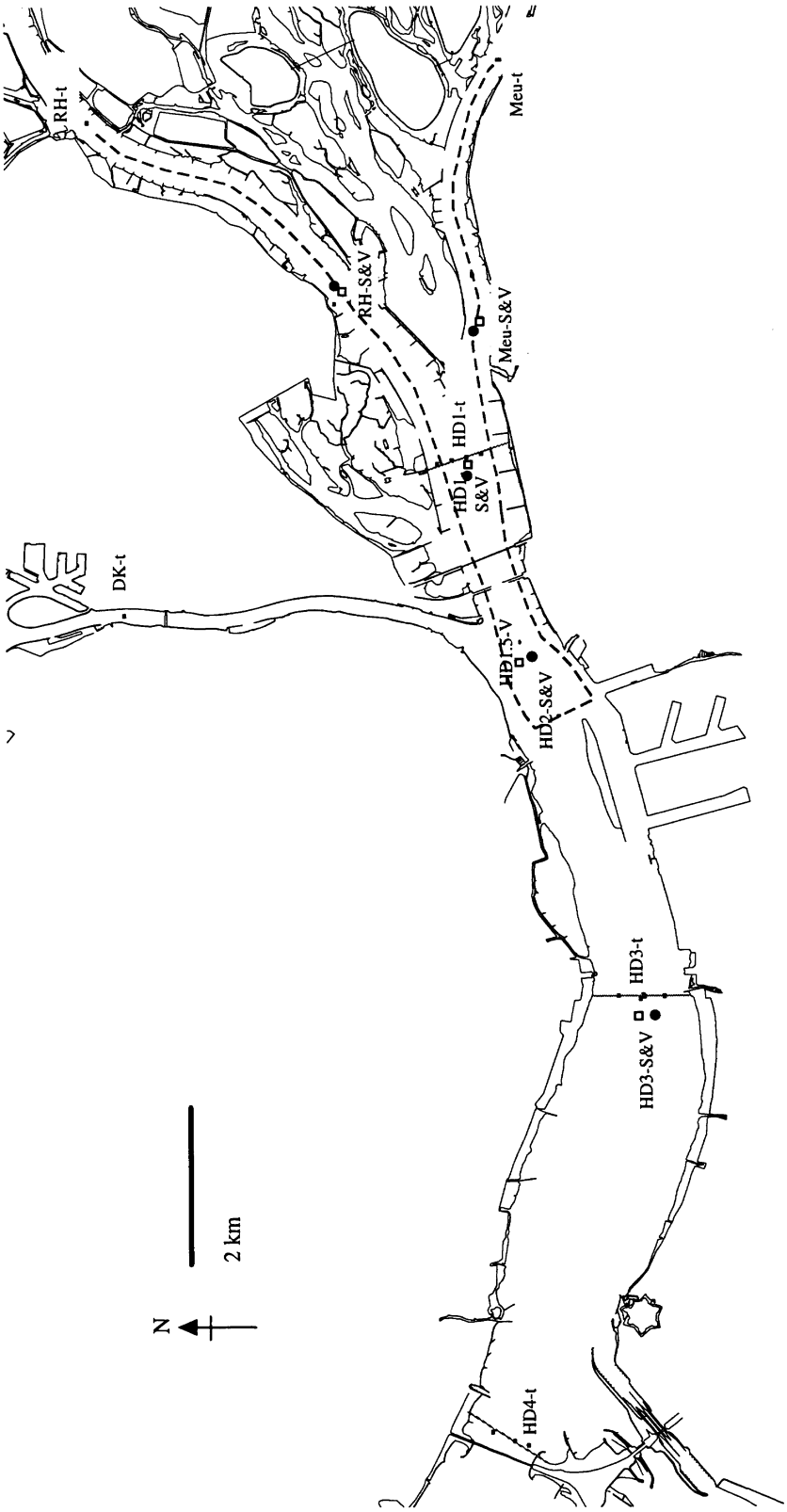

Figure 2. Locations of field survey on 23 and 24 March 1995 in model study area. Explanation of suffixes: –t = measurements of turbidity verticals, represented by filled squares; –V = VIS measurements, represented by circles; –S = ISAC measurements, represented by open squares. The sailed turbidity track is represented by a dashed line

- The hydrodynamic boundary conditions (water levels and discharges) were measured every 10 min at the model boundaries.
- The distribution of suspended sediment throughout the estuary was measured using turbidity probes. At several (constant) positions a vertical turbidity profile was measured each 15 min.
- Turbidity measurements at 1 m below the water surface were continuously taken while sailing. Each day four tracks were sailed, each track taking 2 h. Water samples were taken for all turbidity measurements and the suspended sediment concentration was measured in a laboratory. These were used as calibration data for conversion of the measured turbidity values to suspended sediment concentrations. Unfortunately, due to failure of sampling devices, no grain size measurements on the sampled sediments could be carried out and therefore no information is available with respect to the sand content, organic matter content, etc.
- A floating underwater camera with an incorporated settling tube (Video *In Situ* or VIS) was deployed. With this camera the *in situ* diameter and fall velocity of the suspended particles was measured. A full description of this VIS can be found in Van Leussen and Cornelisse (1993, 1996).
- Air-borne remote sensing images were collected with a JVC S-VHS video recorder at a height of 2500 m on the first day. Two recordings, one of the ebb tidal and one of the flood tidal situation, were taken. As these video recordings are constructed as photographs of the area, they will give an excellent overview of the sediment mixing processes near the water surface. This technique was used for the first time in this area in order to determine suspended sediment concentrations.
- The density of the upper bottom layer (15 cm) was measured on the first day at five different locations. This density profile can be used to estimate the thickness of the fluffy, easily eroded, cohesive sediment layer. This was carried out using an acoustic densitometer. This device, which is called the ISAC (*In Situ* Acoustic Concentration meter), has been shown to be able to measure accurately the excess cohesive bedload thickness when the dry weight is below 750 kg m^{-3}. The method has proven to be more accurate than the traditional echo and sonar sounders (Verbeek and Cornelisse, 1995).

In Figure 2 the measurement locations are shown. The turbidity verticals at the model boundaries were taken on DK-t, RH-t and Meu-t. In the Hollandsch Diep, turbidity verticals were taken on three transects: HD1-t, HD3-t and HD4-t. On each transect, three to four locations were defined, depending on the width of the transect. On each location turbidity verticals were taken every hour throughout the day; no measurements were carried out over night. The moving ship ('sailing') turbidity measurements were taken on a track which is plotted as a dashed line in Figure 2. The bed layer thickness was measured at locations RH-s, Meu-s, HD1-s, HD2-s and HD3-s. The VIS measurements were carried out at locations RH-V, Meu-V, HD1-V, HD1·5-V, HD2-V and HD3-V.

Results and discussion of field survey

Vertical turbidity profiles.

The vertical turbidity profiles were converted to suspended sediment concentrations, using a separate calibration curve for each probe, and integrated over the depth of the profile. The suspended sediment concentration could be predicted within an accuracy of 20 mg l^{-1}. In the results of these measurements, the Rhine boundary (RH-t) shows increasing suspended sediment concentrations during the field survey (from 50 to 90 mg l^{-1}); this is the result of an increasing Rhine discharge. The Meuse boundary (MEU-t) on the contrary carries considerably lower sediment concentrations (15 mg l^{-1}), which hardly change during the field survey.

In Figure 3, time series of the measured suspended sediment concentrations at transect HD1-t and RH-t are plotted as continuous lines. Only the northern- and the southern-most points of transect HD1-t are presented. From this figure it is clear that the concentrations have, particularly on the second day, increased between RH-t and HD1-t, most likely indicating that erosion has taken place between RH-t and HD1. Furthermore, the conclusion can be drawn that Rhine and Meuse water have hardly mixed at HD1-t, because HD1-north has a higher suspended sediment concentration (like the Rhine water) than HD1-south (like the Meuse water). Moreover, a tidal effect is clear at HD1-south. The concentration at this location is changing from the high

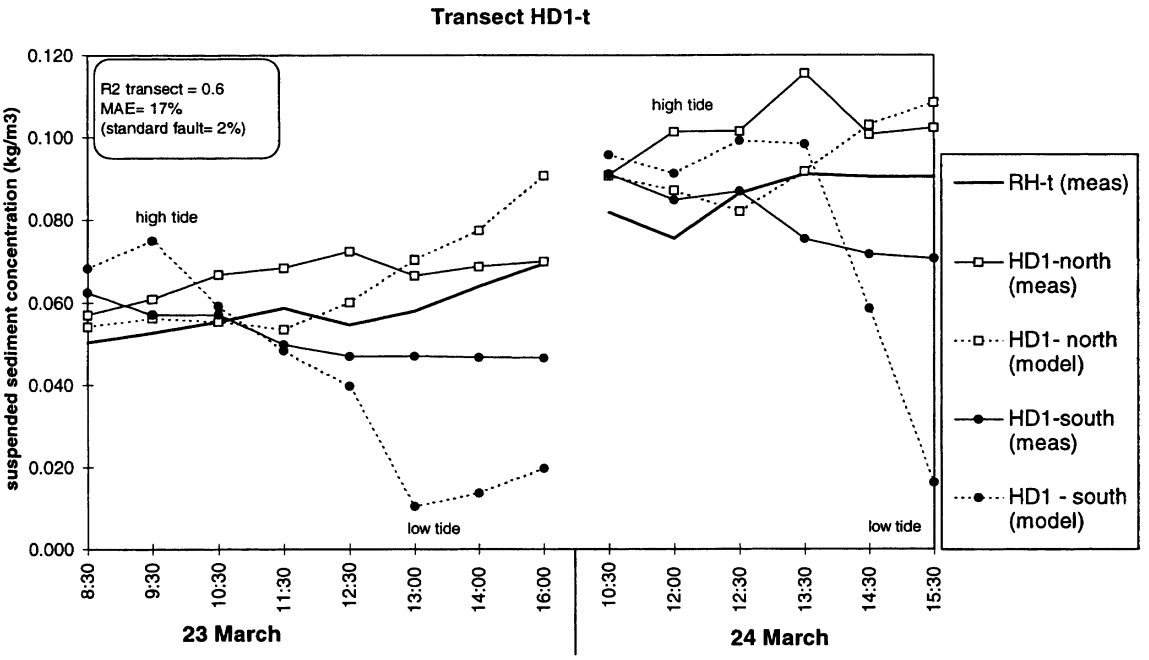

Figure 3. Measured (indicated by (meas)) and modelled (indicated by (model)) suspended sediment concentrations at transect HD1-t

concentrated Rhine water during high tide (most likely this is a situation in which the Rhine is intruding into the Meuse), to the low concentrated Meuse water during low tide. In Figure 3 the periods with high and low tide are indicated.

In Figure 4 the measured concentrations at transect HD3-t are plotted as continuous lines. Again, only the northern- and southern-most locations are presented. The low suspended sediment concentration at HD3-t from 8·00 until 12·00 on 23 March can be attributed to the installation of a new turbidity probe at the end of

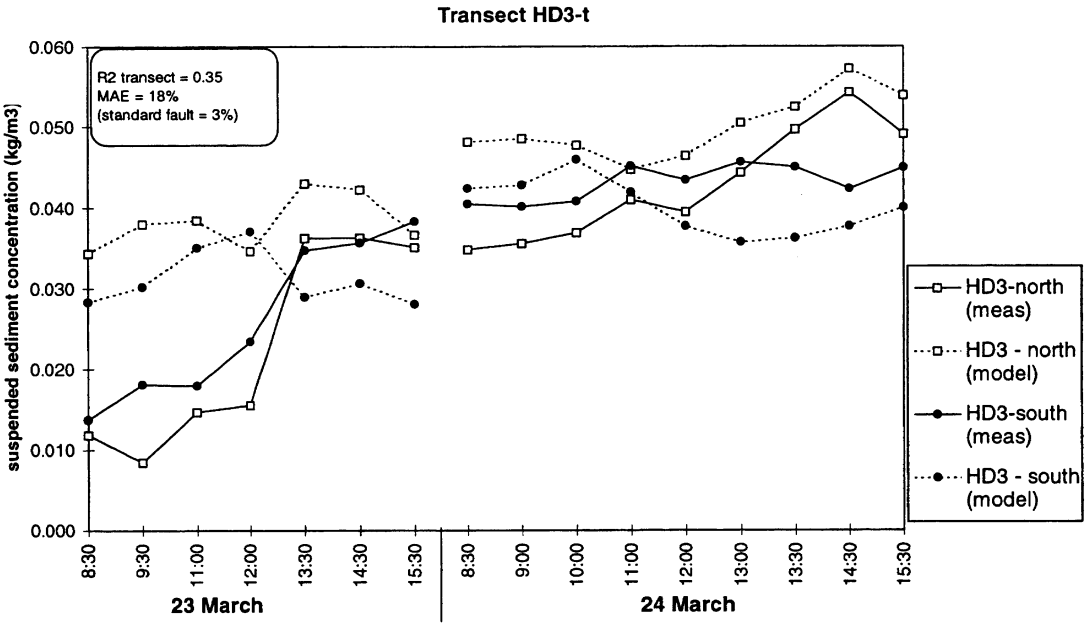

Figure 4. Measured (indicated by (meas)) and modelled (indicated by (model)) suspended sediment concentrations at transect HD3-t

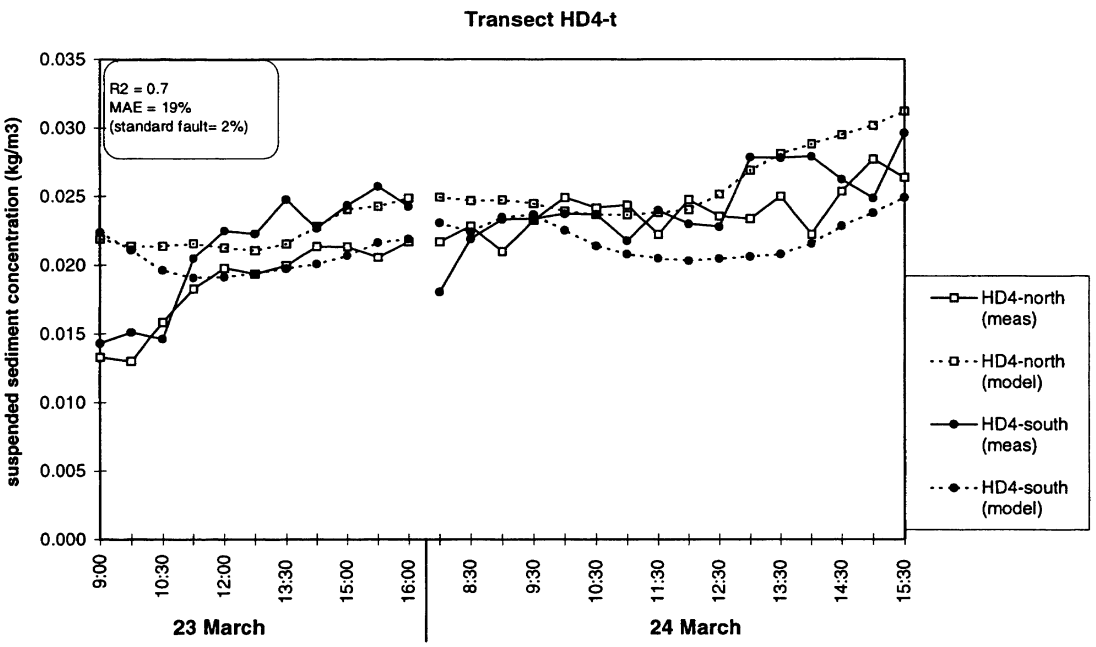

Figure 5. Measured (indicated by (meas)) and modelled (indicated by (model)) suspended sediment concentrations at transect HD4-t

this period. With this second probe the calibration has been carried out, resulting in a poor calibration for the first probe and thus for the first hours. Therefore these values will not be used in model calibration. The difference between the locations at HD3-t comes within the accuracy of the turbidity measurements themselves, therefore it is assumed that the two different streams are mixed at this point. Furthermore, at HD3-t the average suspended sediment concentration is lower than at HD1-t, which indicates that sedimentation occurs between those two transects. This trend appears to continue on to HD4-t (Figure 5, continuous lines) where even lower concentrations (20 mg l^{-1}) were measured.

Remote sensing.

Two remote sensing images were available for use: one of the flood tidal situation (track 1) and one of the ebb tidal situation (track 4). These two coloured images were calibrated to provide information on suspended sediment concentration. This was accomplished using a calibration curve for each image in which the digital values of the coloured pixels were linked to the measured suspended sediment concentrations obtained from the sailing turbidity measurements. For track 1, 3881 observations were available, leading to a calibration curve with a correlation coefficient of 0·55. The standard deviation for this curve is approximately 33 mg l^{-1}. For track 4, 4998 observations were available, leading to a calibration curve with a correlation coefficient of 0·69. The standard deviation for this curve is approximately 12 mg l^{-1}. A detailed description of this calibration exercise is reported in Fraikin and Hartman (1995). The calibration described can be considered to be rather poor and cannot be expected to be useful in a quantitative model calibration. This is checked by comparing the calibrated remote sensing images to the results of the turbidity verticals.

Figures 6a and 7a display the results of these calibrated remote sensing recordings for tracks 1 and 4, which were taken on 23 March at around 10·00 (flood) and 15·30 (ebb) respectively. The concentrations in both Figures 6a and 7a, across the whole area, are indeed preferentially higher than those presented in Figures 3 and 4. Figures 3 and 4 represent the vertically averaged concentrations, whereas Figures 6 and 7 represent the surface concentration. This will not be an issue, as the measured concentration profiles hardly show any curvature, meaning that depth-averaged concentrations are similar to surface concentrations. Because of the

relatively high accuracy of suspended sediment concentrations derived directly from turbidity measurements, compared to a rather poor calibration of the remote sensing images, the concentrations on these photos can be considered too high. This supports the presented conclusion that these images cannot be used quantitatively. However, a qualitative comparison of the model and remote sensing images will be possible.

As observed previously, there is a striking difference in suspended sediment concentration between the northern and southern point of transect HD1-t. The remote sensing images offer more information about this phenomenon. In both Figures 6a and 7a the difference between Rhine and Meuse water and their sediment load is clearly visible. In Figure 6a the situation is flood-tidal, which is illustrated by the Dordtsche Kil flowing towards the southern side of the Hollandsch Diep area and consequently the Rhine water is pushed into the Meuse. In Figure 7a the opposite ebb-tidal situation is illustrated, with water from both the Rhine and Meuse flowing in the western direction and the Dordtsche Kill also flowing in the opposite (northern) direction.

Figure 6a shows that in the upstream area the mixing process proceeds relatively slowly under flood conditions. At the point where the Dordtsche Kil comes out into the Hollandsch Diep area, the mixing of both water streams is accelerated and shortly after this point hardly any difference in suspended sediment concentration remains. Because the effect of the outflowing Dordtsche Kil is not present during ebb (Figure 7a), in this situation the concentration gradient extends further into the Hollandsch Diep and also no Rhine water is pushed into the Meuse.

In Situ Acoustic Densitometer (ISAC).

The ISAC measurements give, through density profiles, an indication of the thickness of the cohesive sediment layer at a specific location. This is particularly interesting information, once flow velocities are high

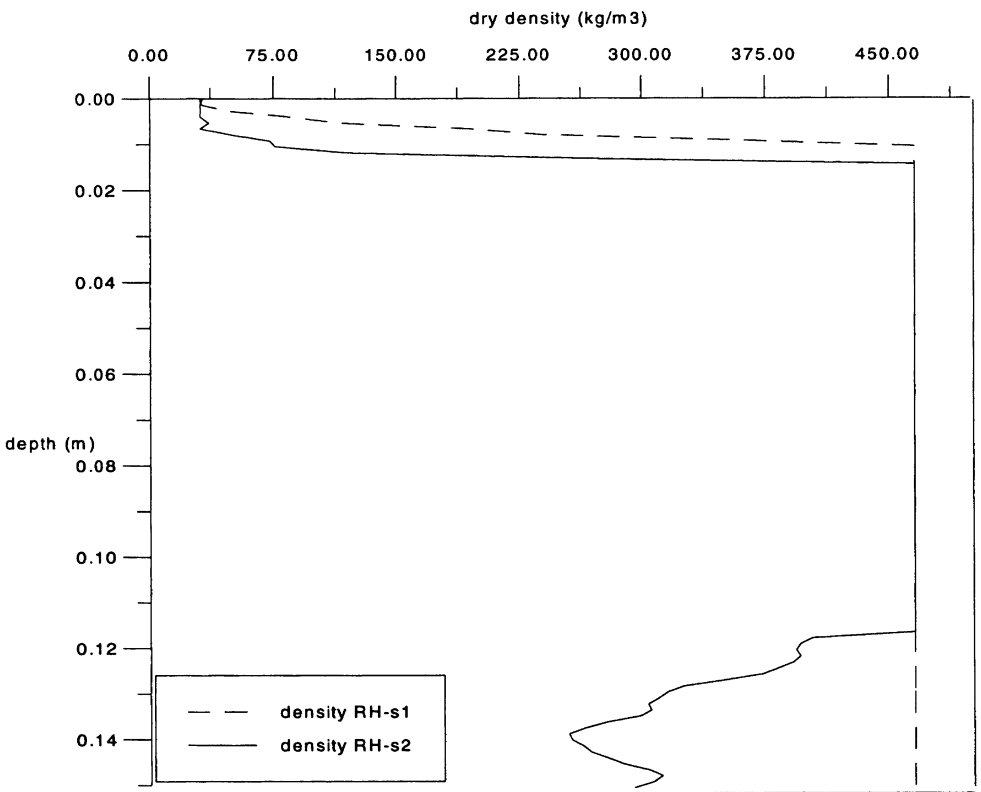

Figure 8. Dry density of bed profile measured with the ISAC at location RH-s1 and RH-s2

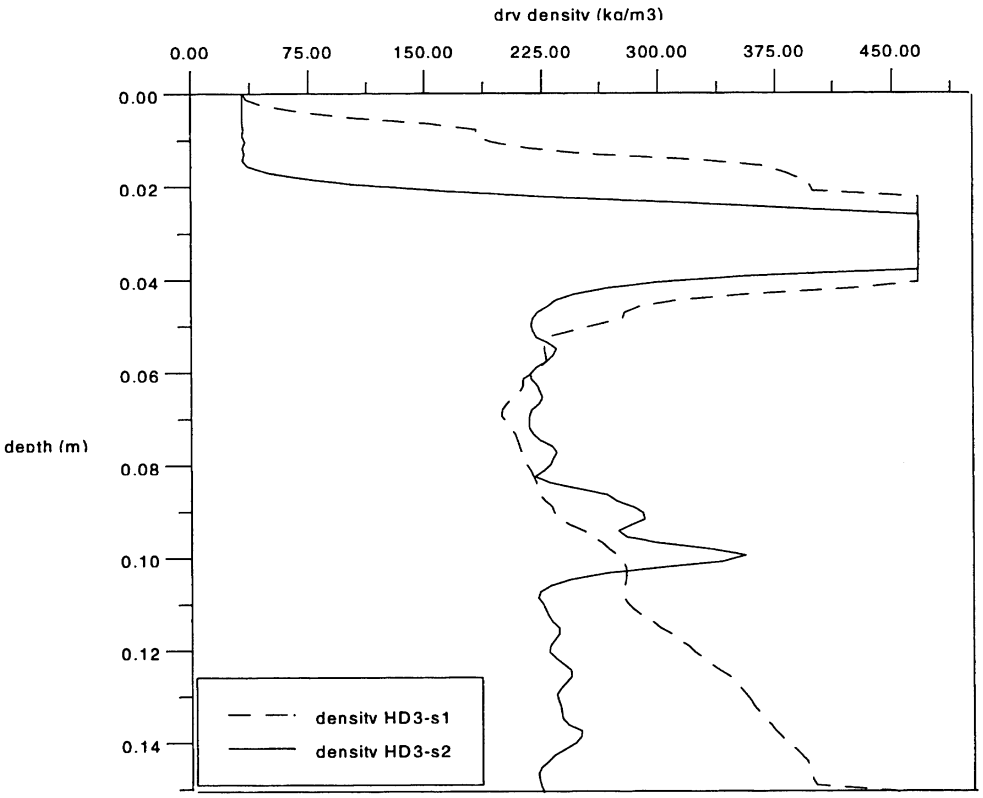

Figure 9. Dry density of bed profile measured with the ISAC at location HD3-s1 and HD3-s2

enough for erosion of these sediments to occur. In Figures 8 and 9 the results for locations RH-s and HD3-s are presented. At both locations two profiles were measured, shown in Figures 8 and 9 with the suffixes −s1 and −s2. The dry density of the non-erodible bed is supposed to be the maximum value in both plots: approximately 450 kg m^{-3}. The accuracy in density is directly linked to the accuracy in the calibration: approximately 50 kg m^{-3}. Both figures show little difference between the −s1 and −s2 profiles. The results indicate the presence of a very thin mud layer estimated at 1 or 2 cm. The profiles measured at the other locations give comparable indications of a relatively thin muddy surface top layer. These data will be used as an initial condition in the model calculations.

Video In Situ (VIS).

During each of the VIS measurements, a 20 min video recording was made, from which for practical reasons only 20 s could be analysed. From these video images, using image analysis software, particle diameter and fall velocity distributions were calculated. The smallest floc which can be detected is restricted by the resolution of the CCD camera and the monitor which are used. This is correlated to the accuracy of the size measurement itself, which is estimated to be around 10 μm. However, factors which are hard to quantify, such as the sharpness of the image, play a role. The accuracy in fall velocity depends strongly on the accuracy of the image algorithm and is estimated to be around 10 μm s^{-1} (Cornelisse and De Jong, 1995).

The main problem in using this instrument appeared to be the internal turbulence in the settling column, induced by the motion of the particles themselves. This resulted in a considerable amount of (probably the lighter) particles having a negative fall velocity (i.e. moving upwards). These were therefore excluded from further analysis. However, because over 60 per cent of all particles remained, these data could be used as an indication of the changes in particle diameter and fall velocity distribution. Especially since the bigger and

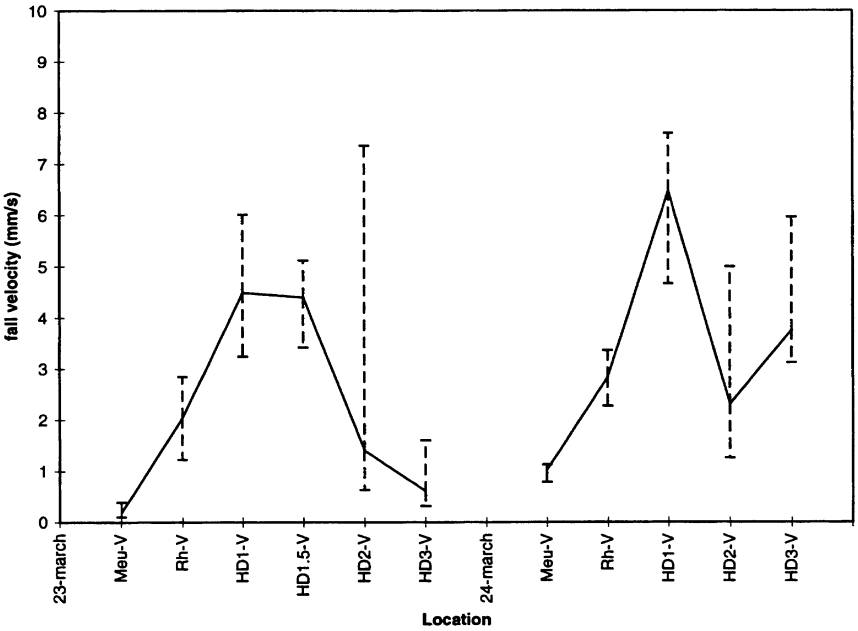

Figure 10. Fall velocity distribution (presented as 50, 75 and 25 per cent values) measured with the *Video In Situ*

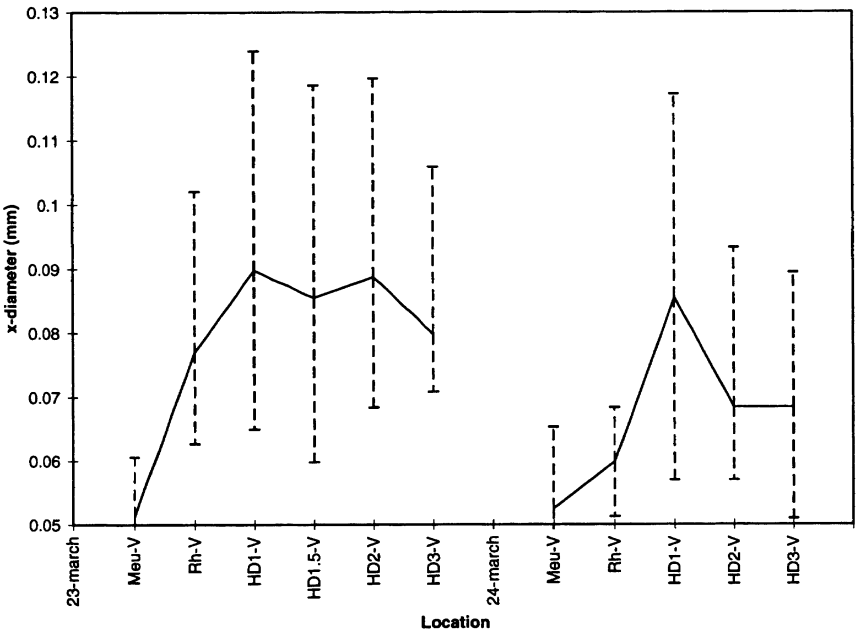

Figure 11. *x* diameter distribution (presented as 50, 75 and 25 per cent values) measured with the *Video In Situ*

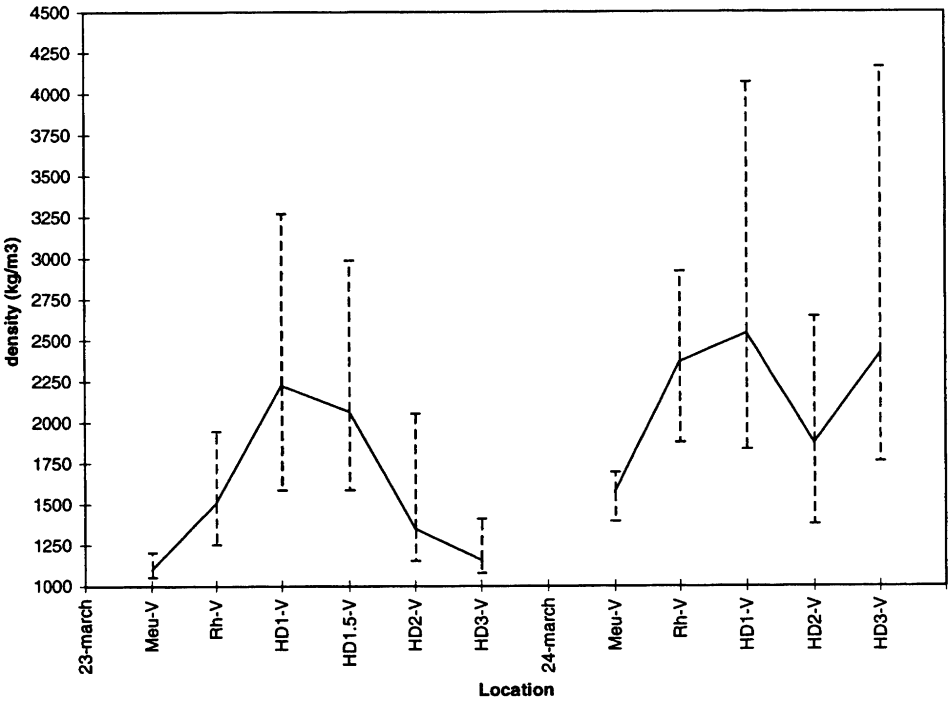

Figure 12. Calculated Stokes equivalent density (presented as 50, 75 and 25 per cent values) from *Video In Situ* data

heavier particles will remain fairly undisturbed in their movements, the transport of sand can be deduced from these data.

The results from the VIS measurements are presented as median values of fall velocity in Figure 10; the error bars present the 25 per cent and 75 per cent reliability interval. The diameter information is presented similarly in Figure 11; the horizontal or x diameter values are presented. From fall velocity and x diameter the equivalent density, using Stokes' law, is calculated; these results are presented in Figure 12. The values in these figures can be compared to other measurements with the same instrument carried out in the same area (Verbeek, 1991), and to measurements carried out with several instruments in the Elbe estuary (Van Leussen and Cornelisse, 1996; Dyer *et al.*, 1996). It is remarkable that, although diameters are fairly small, fall velocities are on average an order of magnitude higher in the measurements presented in this paper than in the papers referred to. This probably indicates the presence of a large amount of sand in the samples, which might be the result of the previously noted turbulence in the settling tube. However, most likely this is at least partly an effect of a suspension with a relatively high sand fraction. A 'normal' situation is reflected in the results at location Meuse-V on the first day, where relatively small particles with a low fall velocity are detected.

On both days a sharp increase in fall velocity occurs between locations RH-V and HD1-V. Since this trend is not observed in x diameter, the calculated density increases as well. After location HD1·5-V, both fall velocity and density decrease. This can be explained by the fact that erosion of sand has taken place between RH-V and HD1-V; it is assumed that densities above (2650 kg m^{-3}) are a result of errors in measurements of both diameter and fall velocity. In previous measurements during a high discharge in 1993 in the same area, Verbeek and Jansen (1993) found high suspended sand contents in the HD1 area (30 per cent). More recently, comparable measurements in the same study area in February 1995 were carried out by van Dreumel (1997), demonstrating erosion of fine sand from the Rhine branch resulting in high sand contents in the HD1-V area. This eroded sand falls out before HD2-V, resulting in lower densities and fall velocities. On the second day the Meuse branch transports more sand and most likely the erosion in the Rhine branch has increased (in

velocity or in area), for the results show finer and denser sediment in all locations. In the downstream area only the light and small mud flocs remain.

CALIBRATION OF THE SEDIMENT TRANSPORT MODEL

Boundary and initial conditions

The measured suspended sediment concentrations at RH-t, DK-t and Meuse-t were used as model boundary conditions. The VIS measurements indicated a relatively high sand fraction in suspension, therefore this was implemented at the model boundaries. Since no direct measurements existed, the size of this fraction was estimated to be 50 per cent. The measured suspended sediment concentrations were divided into the three model fractions: fine sand, flocculated cohesive and fine cohesive. Both cohesive fractions were expected to be of equal size. In this specific situation this led to a ratio of the three fractions of 2:1:1 respectively.

As an initial condition, at the Rhine branch a coarse sediment top layer was used in order to allow erosion of coarse (sandy) material. The ISAC measurements were used to derive the initial condition of thickness of the cohesive bed.

Parameter values

In order to obtain the best possible fit between model and measurements, all parameter values were calibrated. Parameter values from previous studies, carried out in the same study area, concerning one- and two- dimensional modelling of suspended sediment (Verbeek *et al.*, 1995; Van Wijngaarden and Ludikhuize, 1998) and measurements of erosion (Kuijper, 1993; Verbeek *et al.*, 1994), were used as an indication for the order of magnitude. In Table I the parameter values used in the final run are listed. The fall velocities measured with the VIS are an order of magnitude higher than the velocities which are normally used for such a sediment transport model and could therefore not be used, because this would lead to inadequate model calibration.

Table I. Applied parameter values for the sediment transport model ($U_{s,i}$ is the critical depth-averaged flow velocity for sedimentation of fraction i; $W_{s,i}$ is the settling velocity for fraction i; $U_{e,i}$ is the critical depth-averaged flow velocity for erosion of fraction i; M_i is the rate of erosion of fraction i)

Fraction	$u_{s,i}$ (m s^{-1})	$w_{s,i}$ (m d^{-1})	$u_{e,i}$ (m s^{-1})	M_i (kg m^{-2} d^{-1})
Fine sand	0·75	40	0·5	1·0
Flocculated cohesive sediments	0·5	10	0·5	1·0
Fine cohesive sediment	0·25	0·5	0·5	1·0

Model calibration

The WAQUA-DELWAQ model was calibrated quantitatively, using the depth-averaged suspended sediment concentrations from the turbidity profiles measured at transects HD1-t, HD3-t and HD4-t. In a qualitative calibration the remote sensing images were used in order to evaluate whether the spatial distribution on the photos matches the distribution calculated by the model.

Quantitative calibration

The best fit of the model to the measurements was achieved by minimizing the mean sum of squares of the residuals for each transect, as well as averaged for all model results. For an assessment of the model performance two criteria were set:

I. the mean absolute error (MAE) = absolute value of: [(model value −measurement value)/model value], presented as a percentage;

II. R^2 from the (linear) correlation between model results and measurements

In Figures 3, 4 and 5 the results are presented. The dotted lines represent the model results for each location. The concentrations calculated by the model at transect HD1-t match the measured concentrations fairly well; the model results show the same temporal trend ($R^2 = 0{\cdot}6$) and the MAE is 17 per cent. It is notable that the model underestimates the concentration in an ebb-tidal situation at location HD1-south. This is probably the effect of too low suspended sediment concentrations at the Meuse boundary. For transects HD3-t and HD4-t the model results match the measurements, with an MAE around 18 per cent. As an overall model evaluation the MAE is 18 per cent, with a corresponding standard fault of 1 per cent, and R^2 is 0·85.

Qualitative calibration.

The model results were compared qualitatively to the remote sensing images. The model results are presented in Figures 6b and 7b, for 23 March at 10·00 and 15·30 respectively. In both Figures 6a versus 6b and 7a versus 7b the concentrations calculated by the model, throughout the whole study area, are, as expected, lower than those on the corresponding photo. However, the pattern of suspended sediment distribution calculated by the model results resembles the distribution on the remote sensing photographs quite well. Both mixing plumes (outflow Dordtsche Kil and Rhine intruding in the Meuse) from Figure 6a are reproduced adequately in Figure 6b. Figures 7a and 7b are also quite similar in distribution pattern: in both figures mixing only starts in the southwestern area.

CONCLUSIONS AND DISCUSSION

The 2DH model presented is a first attempt to simulate the spatial and temporal distribution of suspended sediment in the southern branch of the Rhine–Meuse estuary. The implemented model equations used are empirically based, but nonetheless the results are promising. For quantitative calibration, depth-averaged suspended sediment concentrations from measured turbidity verticals were used. The model reproduced these measured concentrations quite well, resulting in an overall value for the MAE of 18 per cent, corresponding to, from the upstream to the downstream area, concentrations of about 0·005 to 0·020 kg m^{-3}. The overall R^2 for this run was 0·85.

The model is very sensitive to the partitioning of the three fractions at the model boundary and to the amount of sediment which is eroded. Especially during high discharges, attention must be paid to these phenomena. The calibration of the turbidity measurements must be handled with caution, because the model accuracy is now limited by the accuracy in the turbidity measurements. Given these limitations, the calibrated parameters of this suspended sediment model are in fact only valid for the hydrological situation and geographical area as presented here. However, for each new event, model calibration will be facilitated by the set of parameters which has been derived in this study and in previous studies. If no calibration data are available, this model will at least give a rough estimate of the relevant variables. Moreover, the model will be relevant for use in scenario studies, in which only the relative changes in these variables have to be estimated. A major advantage of a 2DH model compared to a one-dimensional model has proven to be the spatial resolution, whereas both model approaches are equally empirical and show an equal accuracy in the calculation of suspended sediment concentrations (Van Wijngaarden and Ludikhuize, 1998).

The applied aerial remote sensing technique provides a clear qualitative picture of the study area. The pathways of the suspended sediment are clearly visible and are reproduced very well by the model. This means that the dispersion is calculated accurately by the model. It is to be expected that, when using a finer model grid or even a three-dimensional model, the mixing process on the photos can be expected to be reproduced in more detail.

The remote sensing application itself is promising; however, in the future more attention should be paid to the calibration technique. New calibration methods, such as the use of spectral mixture analysis, combined with the measured spectral reflectance of a range of water–sediment mixtures, the so-called endmembers (Mertes *et al.*, 1993), could improve the accuracy. A similar approach could be the complementary use of optical models and calibration data (Dekker *et al.*, 1996).

It has been noted that the fall velocities measured with the VIS are an order of magnitude higher than the velocities which are normally used for such a sediment transport model. This could be explained by the following facts.

- Measurements took place during a period with a relatively high suspended sand transport. Additionally there is no guarantee that the VIS samples were unbiased: as a result of the observed internal turbulence within the settling tube, there might have been an overestimation of heaviest particles. Both factors combined imply that fall velocities might have been relatively high already and also somewhat overestimated.
- The model approach and thus the fall velocities used are valid for a system in which shear stresses are present. The VIS is a device in which shear stress is almost absent. Because shear has a decelerating effect, this might lead to substantially higher fall velocities as measured with the VIS.
- The presence of shear stress and turbulence in the water column induces a continuous process of flocculation and deflocculation, affecting the net fall velocities

In order to use the measured fall velocities, a more physically based model approach is needed in which the sedimentation process is based on a description of (de)flocculation. However, until now no practical description has been found that is useful for large-scale modelling. Attention should also be paid to an instrument with which *in situ*, undisturbed information regarding floc size and fall velocities can be measured.

ACKNOWLEDGEMENTS

The author wishes to thank H. Verbeek for organizing all measurement activities, J. van Zetten for his modelling activities, and S. Fraikin for her support in post-processing the remote sensing recordings. Finally, the captains and crews on board the research vessels are acknowledged for carrying out the measurements.

REFERENCES

Collard, E. A. 1991. A rectilinear WAQUA model for the southern branch of the Rhine–Meuse Estuary: calibration and verification, Document 91·087, Ministry of Transport, Public Works and Water Management, National Institute for Inland Water Management and Waste Water Treatment, Lelystad (in Dutch).

Collard, E. A. 1992. SINODE, A 2DH DELWAQ-model for the southern branch of the Rhine–Meuse Estuary: model specifications and sensitivity analysis, Document 92.104, Ministry of Transport, Public Works and Water Management, National Institute for Inland Water Management and Waste Water Treatment, Lelystad (in Dutch).

Cornelisse, J. M. and De Jong, P. 1995. Video In Situ, Manual VIS-Mk 1, Delft Hydraulics, Report Z161-22/Z960-10, Delft (in Dutch).

Dekker, A. G., Zamurovíc-Nenad, Z., Hoogenboom, H. J. and Peters, S. W. M. 1996. 'Remote sensing, ecological water quality modelling and in situ measurements: a case study in shallow lakes', *Hydrological Science Journal* **41**(18), 531–547.

Delft Hydraulics 1994. DELWAQ User's Manual Version 4·0, Delft.

Dyer, K. R., Cornelisse, J. M. J., Fenessy, M. J., Jones, S. E., Kappenberg, J., McCave, I. N., Pejrup, M., Puls, W., Leussen, W. van Wolfstein, K. 1996. 'A comparison of in situ techniques for estuarine floc settling velocity measurements', *Journal of Sea Research*, **36**(1–2), 15–29.

EDS 1998. User's quide WAQUA, Simona, Report 92-10, Leidschendam.

Elder, J. W. 1959. 'The dispersion of marked fluid in turbulent shear flow', *Journal of Fluid Mechanics*, **5**, 30–41.

Fraikin, S. and Hartman, R. A. 1995. Monitoring of suspended sediment and flow velocity patterns by a video and thermic infrared sensor, Report MDGAR-9549, Geographical Survey Department, Delft (in Dutch.).

Krone, R. B. 1962. Flume studies of the transport of sediments in estuarial shoaling processes, Final Report, Hydrological Engineering Laboratory and Sanitary Engineering, University of California, Berkeley.

Kuijper, C. Cornelisse, J. M. and Winterwerp, J. C. 1993. Erosive behaviour of Haringvliet cohesive sediments, Report Z705, Delft Hydraulics, Delft (in Dutch).

Leendertse, J. J., Langerak, A. and Ras, M. A. M. 1981. 'Two dimensional tidal models for the Delta Works', in Fischer, H. B. (Ed.), Transport Models for Inland and Coastal Waters, Academic Press, New York, 408–450.

Mertes, L. A. K., Smith, M. O., and Adams, J. B. 1993. 'Estimating suspended sediment concentrations in surface waters of the Amazon river wetlands from Landsat images', *Remote Sensing Environment*, **43**, 281–301.

Partheniades, E. 1965. 'A fundamental framework for cohesive sediment dynamics' in Mehta, A. J. (Ed.), Estuarine Cohesive Sediment Dynamics, Coastal and Estuarine Studies 14, Springer-Verlag, Berlin, 219–250.

Van Dreumel, P. F. 1997. Southern branch of the Rhine Meuse Estuary: measurements on suspended sediment and flow velocity during high river discharges of Rhine and Meuse; January/February 1995, Ministry of Transport, Public Works and Water Management,

Directorate Southern Holland, Rotterdam (in Dutch).
Van Eck, G. T. M., Zwolsman, J. J. G. and Saeijs, H. L. F. 1997. 'Influence of compartimentalization on the water quality of reservoirs: lessons to be learned from the enclosure of the Haringvliet estuary, The Netherlands', Proceedings of the Dix-neuvime Congrs des Grands Barrages, Florence, 647–669.
Van Leussen, W. and Cornelisse, J. M. 1993. 'The determination of the size and settling velocities of estuarine flocs by an underwater video system', *Netherlands Journal of Sea Research*, **31**, 321–241.
Van Leussen, W. and Cornelisse, J. M. 1996. 'The underwater video system VIS', *Journal of Sea Research*, **36**(1–2), 77–81.
Van Wijngaarden, M. and Ludikhuize, D. 1998. The impacts of an alternative management of the Haringvliet Sluices on the developments in morphology and waterquality in the Rhine Meuse Estuary, Ministry of Transport, Public Works and Water Management, National Institute for Inland Water Management and Waste Water Treatment, (in Dutch).
Verbeek, H. J. 1991. Measurements with the VIS (Video In Situ) in the Hollandsch Diep and in Lake Volkerak, Document 91·178, Ministry of Transport, Public Works and Water Management, National Institute for Inland Water Management and Waste Water Treatment, Lelystad (in Dutch).
Verbeek, H. J. and Jansen, B. 1993. High discharge in the Meuse: suspended sediment meausurements in the Rhine Meuse estuary, Document 93·141, Ministry of Transport, Public Works and Water Management, National Institute for Inland Water Management and Waste Water Treatment, Lelystad (in Dutch).
Verbeek, H. J., Sileon, M. E. and van Zetten, J. W. 1993. A WAQUA-DELWAQ TEMPERATURE MODEL for the southern branch of the Rhine Meuse estuary calibrated on the 4^{th} of July 1991, Document 92·065, Ministry of Transport, Public Works and Water Management, National Institute for Inland Water Management and Waste Water Treatment, Lelystad (in Dutch).
Verbeek, H. J., Jansen, B. and Van Zetten, J. 1994. Measuring erosion in the Haringvliet area during a high discharge (December 1993), Report 94·044, Ministry of Transport, Public Works and Water Management, National Institute for Inland Water Management and Waste Water Treatment, Lelystad (in Dutch).
Verbeek, H. and Cornelisse, J. M. 1995. 'Consolidation of dredged sludge, measured by an acoustic densitometer', *Marine and Freshwater Research*, **46**, 179–188.
Verbeek, H. J., Van Zetten, J. and Ludikhuize, D. 1995. A comparison between 1D and 2D sediment transport models for the southern branch of the Rhine Meuse estuary, Document 95·107, Ministry of Transport, Public Works and Water Management, National Institute for Inland Water Management and Waste Water Treatment, Lelystad (in Dutch).

